

## Heat Transfer Based Scale-Down of Chemical Reactions

Edward Mark Davis\* and Shekhar Krishna Viswanath

Chemical Product R&amp;D, Eli Lilly &amp; Co., Lilly Corporate Center, Indianapolis, Indiana 46285, United States

## Supporting Information

**ABSTRACT:** Mathematical models of dose controlled reactions based on heat flow data<sup>1,2</sup> are quite common and well developed; however, such predictions for nondose controlled reactions from heat flow data are difficult, requiring extensive study of the kinetics of multiple chemical transformations as well as physical phenomena such as dissolution and diffusion. Presented here is a new scale-down methodology to directly observe, in the laboratory, a variety of dose controlled and nondose controlled large scale thermal effects. This experiment-based scale-down approach has been derived mathematically from first principles, as well as demonstrated experimentally. This approach limits the heat transfer of the laboratory reactor to the scale equivalent of the intended large scale vessel by dynamic jacket set points based on the ratio of the heat transfer coefficients of lab and plant scale reactors. This allows large scale reaction temperature and other temperature-related effects to be mimicked on small scale while maintaining the time/reaction temperature response profile of the large scale vessel in the laboratory. The result is a method for the direct observation, in the laboratory, of the scale-up effects of changing a wide range of process variables for both dose controlled and non-dose controlled systems. Applications for this methodology could include evaluating the effects of proposed large scale process changes on process safety, product purity, or product physical properties as well as evaluating the effects of failure scenarios.

## INTRODUCTION AND LITERATURE REVIEW

In general, reaction calorimetry can be segmented into two basic methods: heat flow and power compensation. Power compensated calorimetry applies a known heat flow into the reactor via an immersed heater. With the jacket fluid flow rate and temperature held constant, any change in reaction temperature invokes an increase or decrease in the heater output to compensate and maintain the reaction at the set reaction temperature. Thus, the heat flow of the reaction is measured directly as the change in heat applied through the compensation heater. Heat flow calorimetry, on the other hand, uses a calibration heater to calibrate the heat flow across the jacket before and after the reaction takes place. The calibration heater is energized from time = 0 to time =  $t$ . The heat transfer coefficient times area ( $UA$ ) is calculated from eq 1.

$$\int_0^t Q_{\text{cal heater}} = UA \int_0^t (T_r - T_j) \quad (1)$$

Once  $UA$  is known, then the same equation is used to measure an unknown heat of reaction

$$\int_0^t Q_{\text{flow}} = UA \int_0^t (T_r - T_j) \quad (2)$$

$$Q_{\text{Rxn}} = Q_{\text{flow}} + Q_{\text{accu}} + Q_{\text{loss}} + Q_{\text{dose}} \quad (3)$$

The region of interest (unknown thermal event) must be bracketed with a calibration  $UA$  measurement before and after. It must be assumed that the change in the resulting  $UA$  measurements is constant over time or proportional to some reaction variable such as reaction completion.<sup>3</sup>

Traditional reaction calorimetry is typically done isothermally to zero out the term for the accumulated heat of the reaction ( $Q_{\text{accu}}$ ).  $Q_{\text{loss}}$  is the heat loss to the environment and can be estimated.  $Q_{\text{dose}}$  is the heat required to change the

temperature of the dosed reagent to the reaction temperature. This can be calculated from the mass of the dose and the heat capacity of the dose.<sup>4</sup> Once all the contributing  $Q$  terms are known,  $Q_{\text{Rxn}}$  (heat of reaction) can be easily calculated in postprocess mode. Most reaction temperatures deviate a few tenths of a degree centigrade from the set point over the course of the reaction, as a typical calorimeter has extremely good heat transfer. Typically large scale reactors cannot accomplish this level of temperature control, making direct scale-down of temperature profiles for large reactions impossible under normal calorimeter control modes.

Mathematical models for reaction scale-up utilizing heat of reaction profiles from a reaction calorimeter ( $Q_r$  models) are commonly used and will not be discussed in detail here. These are quite accurate and predictive for simple dose controlled reactions. In the case of a dose controlled reaction, the model can be time stretched or shrunk to predict the effects of various addition rates on the batch temperature profile. The model only remains valid as long as the originally measured heat of reaction profile is valid, i.e., as long as the full potential heat of reaction from the addition of any reagent is immediately expressed as a change in reaction temperature. Care must be observed when shrinking the time frame of these models (looking at the effects of decreased addition times) that dose control is confirmed by experimentation at the shorter addition time. These simple models cannot predict changes in reaction rates or byproduct formation without extensive knowledge of the complete reaction kinetics, including alternative reaction pathways and side reactions.

Recently, Niemeier<sup>5</sup> developed a scale-down method to mimic large scale vessels in a calorimeter during dosing

Received: February 8, 2012

Published: June 14, 2012

Table 1. Comparison of Scale-Up and Scale-Down Methods

scale-down calorimetry	traditional reaction calorimetry	heat transfer computer models (qr models)
<ul style="list-style-type: none"> <li>simulation is run at real-life temperature profile</li> <li>mimics dose and nondose controlled reactions</li> <li>able to handle physical property changes during reaction</li> <li>heat transfer coefficient and area can be constantly updated based on real time measurements.</li> </ul>	<ul style="list-style-type: none"> <li>force constant reaction temperature therefore does not predict behavior resulting from batch temperature changes</li> <li>measures dose and nondose controlled reactions usually isothermally by direct experimental measurement</li> <li>able to handle physical property changes during reaction with advanced options</li> <li>temperature dependent changes in heat transfer coefficient or specific heat capacity are not seen during isothermal runs</li> </ul>	<ul style="list-style-type: none"> <li>works well for dose-controlled reactions run isothermally</li> <li>purely heat transfer models predict dose controlled behavior only</li> <li>limited ability to handle physical property and temperature changes of reaction mixture</li> <li>temperature dependent changes in heat transfer coefficient or specific heat capacity must be measured and accounted for</li> </ul>

operations. In this method, the dosing of the reagent is set to be suspended when the heat transfer across the jacket exceeds a value predetermined from the heat transfer capabilities of the large scale vessel. This allows a chemical process with unknown heat of reaction to be executed over the same time frame as will occur on scale. This is most easily accomplished with a calorimeter able to directly measure heat flow such as the Mettler Toledo RTCal system or with a power compensation calorimeter.<sup>6</sup> (The RC1 with RTCal option is a reaction calorimeter manufactured by Mettler-Toledo.) Highly accurate complex dosing strategies can be taken directly from the mass versus time curve of a lab experiment run under these conditions simply by multiplying the lab dosing mass by the scale-up factor. It is unnecessary to apply a scale factor to the time scale of the curve. This method cannot handle reaction temperature changes not reflected in the lab scale run and is only applicable to dose controlled reactions.

Another experimental scale-down approach was developed and patented by Zufferey and co-workers.<sup>7,8</sup> Their approach was to calculate the heat released in a lab reactor during a small time interval. This heat value was multiplied by the scale factor to determine the large scale heat of reaction. The amount of energy removed by a theoretically calculated large scale jacket was subtracted, and a new theoretical large scale reaction temperature change was calculated. The batch temperature set point of the reaction calorimeter is then changed to the new calculated large scale reaction temperature. This involves many calculations of the heat of reaction and reaction temperature over a small unit of time. Zufferey states

$$q_{rx}^{RC1}(k) = m_r^{RC1} C_p^{RC1} \frac{\Delta T_r^{RC1}}{\Delta t} + UA(T_r^{RC1}(k) - T_a^{RC1}(k)) - \frac{m_r^{RC1}(k) - m_r^{RC1}(k-1)}{\Delta t} C_{p_{dose}}^* (T_{dose} - T_r^{RC1}(k)) - \alpha(k) T_{amb} - T_r^{RC1}(k) \quad (4)$$

Using the result of eq 4, Zufferey calculated the temperature change over the time segment on scale using eqs 5 and 6.

$$\frac{\Delta T_{scale}}{dt} = \frac{S_f * q_{RC1} - UA(T_{r_{scale}} - T_{j_{scale\ calc}})}{m_{scale} C_p} - q_{dose} - q_{loss} \quad (5)$$

$$T_{set\ RC1} = T_{r_{set\ previous}} + \Delta T_{scale} \quad (6)$$

The calculations depicted in eqs 4, 5, and 6 are updated every 10 s. Each of the terms in eqs 4 and 5 contribute error to the  $\Delta T_{scale}$  calculation.

Our scale-down method is fundamentally different in that we eliminate much of the compounded calculation error by allowing the system itself to perfectly “calculate” reaction

temperature by restricting the heat flow across the RC1 jacket to the scaled down equivalent of the large scale vessel. We eliminate the additive and compounding error inherent in attempting to calculate a  $\Delta Tr$  through multiple heat flow calculations for both the large and small vessels by directly utilizing predicted large-scale jacket temperature values to calculate RC1 jacket temperatures on the basis of a heat transfer scale-down model and the current reaction temperature, completely eliminating the need for heat flow data and a calorimeter.

In summary, mathematical models can be used in combination with experiments either in postprocess mode to facilitate scale-up predictions, or concomitantly within the experiment to enable a true temperature profile scale-down of the reaction. Use of a true scale-down approach allows predictions of impurities, side reactions, gas evolution, or other mal-events through direct laboratory observation and analysis of the in-process or completed reactions without any foreknowledge of reaction kinetics. Table 1 shows a comparison of scale-up and scale-down methods currently utilized in the pharmaceutical industry. Using a scale-down approach, it is possible early in the route selection or process development of a target to demonstrate manufacturability for a proposed synthetic step or route. This scale-down method has been utilized by Lilly to predict the manufacturability of large scale clinical runs of a highly complex, one pot, multiple step, multiple solid and liquid phase reaction, while research into a full kinetic understanding of the mechanism and intermediate solubilities involved was just getting underway.

It is important to emphasize that our scale-down method does not require a calorimeter and can be performed in any computer-controlled, physically well-characterized jacketed reactor that is capable of accurately measuring reaction and jacket temperatures and can react to rapid jacket set point changes.

## ■ MATHEMATICAL FORMULATION OF THE SCALE-DOWN APPROACH

The basis of our scale-down approach is scale-up first principles in reverse. Since it is accepted that scale-up behavior can—within limits—be predicted from small scale heat, mixing, and heat transfer data, it follows conversely that, restraining the heat transfer of a laboratory reactor to the mole proportional equivalent of the large scale vessel while maintaining equivalent mixing will allow direct observation of large scale temperature profile and reaction behavior in the laboratory vessel.

**List of Assumptions.** (1) Reaction starting temperatures of lab and scale are the same.

(2) The reaction temperature is well below the boiling point of the reaction mixture such that  $Q_{loss}$  in the lab reactor is small

and nearly constant at temperatures near the desired batch temperature.  $Q_{\text{loss}}$  in the scale vessel is negligible.

(3) All raw material quantities are scaled down in the lab reactor by the reciprocal of the scale factor as defined in eq 8.

(4) All time values in the lab reaction (addition time, etc.) are identical to those in the large scale run.

(5) Mixing equivalence is assumed between the lab vessel and the large scale vessel. A discussion of this assumption can be found under the heading "Calculation of the Heat Transfer Coefficient " $U_{\text{scale}}$ " from a  $U_{\text{lab}}$  Measurement".

(6) The value of all variables is held constant at the starting value of each  $T_{j,\text{lab}}$  calculation time segment ( $dt$ ). This is based on the assumption that the change in value of the variable will be small compared to the absolute value of that variable. This assumption will also be discussed in the mathematical derivation section. This assumption must be carefully applied to very rapidly changing systems.

**First Principles Derivation.** As with Zufferey's method, we break the reaction into small discrete time segments to simplify the treatment of temporally changing variables during individual calculation steps. Each calculation is informed by the previous calculation to account for any change in the value of the variables since the last calculation. Whereas Zufferey goes on to do  $Tr_{\text{scale}}$  calculations based on discrete energy output measurements from a reaction calorimeter, our method solves an equivalent equation for a laboratory reactor jacket set point, thereby allowing the reaction itself to "calculate" the batch temperature.

The basic energy balance equation (eq 3) for a dosed reaction can be stated as the heat of the chemical reaction equals the heat of dosing plus the heat flow across the jacket plus the heat accumulated in the reaction and heat lost from the jacket to the atmosphere.

$$Q_{\text{Rxn}} = Q_{\text{accu}} + Q_{\text{dose}} + Q_{\text{flow}} + Q_{\text{loss}} \quad (3)$$

Basic scale up principles dictate that, for any fixed set of reaction conditions, the values of  $Q_{\text{R}}/\text{mole}$  and  $Q_{\text{dose}}/\text{mole}$  are independent of scale.

Let us neglect  $Q_{\text{loss}}$  as insignificant for a moment. In practical application, we will later add back a "calibration factor" which will account in part for this term as well as some other factors. We can then solve for the accumulated heat term.

$$Q_{\text{accu}} = Q_{\text{rxn}} - Q_{\text{dose}} - Q_{\text{flow}} \quad (7)$$

Let us define the molar ratio of the two scales as  $Sf$ .

$$Sf = \frac{\text{moles}_{\text{scale}}}{\text{moles}_{\text{lab}}} \quad (8)$$

Now let us propose the design of a reaction system in the lab vessel such that

$$Q_{\text{accu lab}} * Sf = Q_{\text{accu scale}} \quad (9)$$

By causing the equality in eq 9 by our hybrid method of experimental design and calculation, we cause the change in temperature of the reaction masses of both the large and small vessels to be identical. Thus, if we start the reactions at the same temperature, the final reaction temperatures will also be identical.

On the basis of eqs 7,8, and 9, we can set up the following equality:

$$\frac{Q_{\text{rxn lab}} - Q_{\text{dose lab}} - Q_{\text{flow lab}}}{Q_{\text{rxn scale}} - Q_{\text{dose scale}} - Q_{\text{flow scale}}} = Sf \quad (10)$$

Because our goal is not to just make the final reaction temperature of the scale and lab reactors equal but to maintain that equality throughout the entire course of the reactions, we must define our experimental conditions such that eq 10 is valid not only for the reaction as a whole but also for any given moment in time during the course of the reaction. This can be represented by the conditions set forth in eqs 11–14.

$$\frac{dQ_{\text{rxn lab}}}{dt} = \frac{dQ_{\text{rxn scale}}}{dt} * \frac{1}{Sf} \quad (11)$$

The equality in eq 11 can be accomplished by assuring all reagents and solvents are scaled according to eq 8, by maintaining the same time scale for both large and small reactions, and maintaining  $Tr_{\text{lab}} = Tr_{\text{scale}}$ ; this last condition shall be discussed later.

$$\frac{dQ_{\text{dose lab}}}{dt} = \frac{dQ_{\text{dose scale}}}{dt} * \frac{1}{Sf} \quad (12)$$

Again, the equality in eq 12 can be accomplished by assuring all reagents and solvents are scaled according to eq 8, by maintaining the same time scale for both large and small reactions, maintaining the same dosing temperature for both scales and maintaining  $Tr_{\text{lab}} = Tr_{\text{scale}}$ .

$$\frac{dQ_{\text{flow lab}}}{dt} = \frac{dQ_{\text{flow scale}}}{dt} * \frac{1}{Sf} \quad (13)$$

Maintaining the equality in eq 13 is the heart of our scale-down method. To do this we will calculate a series of laboratory jacket temperatures such that the heat flow across the lab reactor jacket is exactly  $1/Sf$  that of the large scale vessel at the same point in the reaction.

$$\frac{dQ_{\text{accu lab}}}{dt} = \frac{dQ_{\text{accu scale}}}{dt} * \frac{1}{Sf} \quad (14)$$

The equality given in eq 14 follows from setting the reaction conditions to satisfy eqs 10–13 (A mathematical proof that, by satisfying eqs 10–14, the relationship  $Tr_{\text{scale}} = Tr_{\text{lab}}$  will hold true at all points of time during the lab and scale reactions can be found in the Supporting Information.) and results in the relationship

$$Tr_{\text{scale}} = Tr_{\text{lab}} \quad (15)$$

Thus, the lab and scale reaction temperatures can be held identical for all points in time over the course of the reaction. Because of the relationships established in eqs 10–14, we can write

$$\frac{dQ_{\text{rxn lab}}}{dt} - \frac{dQ_{\text{flow lab}}}{dt} - \frac{dQ_{\text{dose lab}}}{dt} = \left( \frac{dQ_{\text{rxn scale}}}{dt} - \frac{dQ_{\text{flow scale}}}{dt} - \frac{dQ_{\text{dose scale}}}{dt} \right) * \frac{1}{Sf} \quad (16)$$

In summary, if we can design an experiment to satisfy eq 13, then it follows mathematically from eq 16 that eq 14 must be satisfied. Restated, if we can hold, through experimental design, the  $Q_{\text{dose}}$  and  $Q_{\text{rxn}}$  terms of the lab reactor proportional by  $1/Sf$

at all times and then calculate a series of lab jacket temperatures such that the lab reactor heat flow is  $1/Sf$  of the large reactor heat flow at all times, then the accumulated heats and thus the reaction temperatures will be exactly equal at all times. Proceeding from the confidence that a lab reaction can be designed to satisfy our basic assumptions and eq 16, we propose to derive a continuously updating  $T_{j\text{lab}}$  calculation that meets the goal of controlling  $Q_{\text{flow}}$  in the lab to  $1/Sf$  of the large scale reactor (eq 13) at any time during the entire course of the reaction. To perform these calculations, we must hold temporally changing values such as reaction temperature, mass, and volume constant during our calculation update time ( $dt$ ) (see basic assumption no. 6), we must select a small “ $dt$ ” or calculation time segment such that the change in value of the temporally changing variables can be considered negligible compared to their absolute value and thus can be ignored without causing unacceptable error. Time-dependent variables such as volume and mass are held constant during each jacket temperature calculation time increment and updated with current values prior to the calculations for the next time increment. Thus, in eq 17, we select a value for  $dt$  such that the difference between the end and start values of each changing variable is small relative to the absolute value of the measured parameter. If this cannot be reasonably achieved, the method should not be used.

We start by expressing the  $Q_{\text{flow}}$  term of eq 16 in terms of its fundamental relationships to kinetic, thermodynamic, and physical properties. Thus, for any moment in time,

$$\frac{dQ_{\text{flow}}}{dt} = UA(Tr - Tj) \quad (17)$$

Going back to eq 13 and substituting the equality in eqs 15 and 17, we derive eq 18.

$$Sf * UA_{\text{lab}}(Tr - T_{j\text{lab}}) = UA_{\text{scale}}(Tr - T_{j\text{scale}}) \quad (18)$$

It is interesting to note that many of the temporally changing variables that are required to be measured and inputted into the Zuffery eq 4 do not appear in our calculations because we take advantage of experimental design to cause them to algebraically cancel out from eq 16, leaving only the  $Q_{\text{flow}}$  terms behind to contribute to eq 18. This is caused by an experimental design that assures scale dependent variables are proportional for any random time slice of the reaction. Scale independent variables being of equal value on each side of the equation due to making the time scales equal must cancel out of the equality at this point as well. This is not to say these variables are ignored or otherwise neglected by our method but rather that the method carries these variables within the lab reaction itself, eliminating measurement and calculation errors. This is part of the simple elegance of our method over previous methods. In essence, we allow the reaction itself to “calculate” and perfectly maintain the values of many temporally changing variables over the course of the reaction.

Because we wish to know how to control  $T_{j\text{lab}}$  so that the equality of eq 13 will be satisfied, we solve eq 18 for  $T_{j\text{lab}}$ . This provides our basic scale-down eq 19, which in practice is recalculated every 5 to 10 s using updated reaction values from the lab reactor software.

$$\frac{(Sf * UA_{\text{lab}} - UA_{\text{scale}})}{Sf * UA_{\text{lab}}} Tr + \frac{(UA_{\text{scale}} T_{j\text{scale}})}{Sf * UA_{\text{lab}}} = T_{j\text{lab}} \quad (19)$$

It is important to keep in mind that eq 19 describes the calculation of the  $Tj$  set point from values reported at the end of the last time segment. This new  $Tj$  set point is sent to the reactor software, after which all variables are updated and a new  $Tj$  set point is calculated to be sent out at the next update. It is in this way we account for the accumulation of mass and concomitant changes in reaction volume and heat transfer area from any ongoing dosing operation, but this can introduce some delay error, especially in very rapidly changing systems.

**Adjustment for Lab Vessel Calibration.** A correction is required to compensate for the small measured temperature difference between batch temperature and jacket temperature when the lab vessel is at thermal equilibrium. This difference is the sum of the  $Tr$  and  $Tj$  thermocouple calibration errors and  $Q_{\text{loss}}$ , which is heat lost to the environment. Despite neglecting the  $Q_{\text{loss}}$  term to arrive at eq 7 from eq 3, this term can be significant, especially at temperatures close enough to the boiling point of the reaction mixture to cause condensation to form above the reaction surface and on the reactor head. The difficulty involved in relating the lab and plant values of this term is why we make assumption no. 2—the assumption that the reaction temperature is well below reflux. Given this constraint, we propose that this correction is only necessary for the lab vessel and not the scale-up vessel (heat losses are proportional to surface area/volume). The  $Q_{\text{loss}}$  on scale is expected to be orders of magnitude smaller than the other  $Q$  terms on the scale side of eq 3.

We define the variable “ $C$ ” for a calibration factor, where

$$C = Tr - Tj \quad \text{when} \quad \frac{dTr}{dt} = 0 \quad \text{and} \quad Q_{\text{R}} = 0 \quad (20)$$

“ $C$ ” is temperature dependent because of the contribution of  $Q_{\text{loss}}$  but if we keep the reaction temperature change to a minimum, the change in  $Q_{\text{loss}}$  will be small, keeping the error relatively small. Thus,  $C$  can be approximated by equilibrium measurement of  $Tr - Tj$  at the chosen reaction temperature or an average projected experiment temperature. The constant  $C$  is determined prior to the start of the experiment and is maintained as a constant numerical value throughout the scale-down experiment. Applying “ $C$ ” to the scale-down equation (eq 19) results in eq 21.

$$\frac{(Sf * UA_{\text{lab}} - UA_{\text{scale}})}{Sf * UA_{\text{lab}}} Tr + \frac{(UA_{\text{scale}} T_{j\text{scale}})}{Sf * UA_{\text{lab}}} - C = T_{j\text{lab set}} \quad (21)$$

**Dynamic Heat Transfer Area Calculation.** A correction for the heat transfer area of the large vessel “ $A_{\text{scale}}$ ” is derived from the equations for the volume and surface area of the cylindrical portion of the scale reactor and the volume relationship to density and mass for the dosing. Given the basis of this calculation, all large scale reactions must have a starting volume sufficient to completely fill the bottom dish of the scale reactor. Also, these calculations assume a vertical wall reactor. Other geometries are easily incorporated into the formulation of eq 22 for noncylindrical reactors. In eq 22, we capture the relationship between accumulating reaction mass and volume due to the dosing event as a change in  $A$  (the heat transfer area) with each new calculation by utilizing the following mathematical relationship:

$$\Delta A_{\text{scale}} = \frac{2 * Sf \Delta m_{\text{lab}}}{d * r} \quad (22)$$

where  $d$  is the density of the dosed material and  $r$  is the radius of the large scale vessel.  $\Delta m_{\text{lab}}$  is informed by update from the instrument controller software at the end of the previous time slice calculation. In this manner, the cumulative nature of the dosed mass is captured as increasing reaction mass, volume, and heat transfer area during each successive  $T_j$  calculation. Thus, given eq 30,  $A_{\text{scale}}$  for each successive calculation is defined as

$$A_{\text{scale new}} = A_{\text{scale previous}} + \frac{2 * Sf * \Delta m_{\text{lab}}}{d * r} \quad (23)$$

To simplify the calculation visually, we define a constant  $Z$ .

$$Z = \frac{2 * Sf}{d * r} \quad (24)$$

Substituting  $Z$  into eq 23.

$$A_{\text{scale}} = A_{\text{scale start}} + Z \Delta m_{\text{lab}} \quad (25)$$

Using the equality established in eq 25, substitute for  $A_{\text{scale}}$  in eq 21.

$$\frac{(Sf * UA_{\text{lab}} - (U_{\text{scale}}(A_{\text{scale start}} + Z \Delta m_{\text{lab}})))}{Sf * UA_{\text{lab}}} Tr + \frac{(U_{\text{scale}}(A_{\text{scale start}} + Z \Delta m_{\text{lab}}) T_{j_{\text{scale}}})}{Sf * UA_{\text{lab}}} - C = T_{j_{\text{lab set}}} \quad (26)$$

Simplify:

$$T_{j_{\text{lab}}} = \left[ 1 - \frac{U_{\text{scale}}(A_{\text{scale start}} + \Delta m Z)}{Sf * UA_{\text{lab}}} \right] Tr + \frac{U_{\text{scale}}(A_{\text{scale start}} + \Delta m Z)}{Sf * UA_{\text{lab}}} T_{j_{\text{sc}}} - C \quad (27)$$

The use of eq 27 to control the jacket set point of the lab reactor assumes that  $A_{\text{lab}}$  is also calculated in real time from the dosed mass and dose density. RC1 software does this automatically and sends the new value to the calculation spreadsheet to be incorporated in the next  $T_j$  set point calculation.

**Calculation of the Heat Transfer Coefficient  $U_{\text{scale}}$  from a  $U_{\text{lab}}$  Measurement.** The overall heat transfer of a system can be expressed as the inverse of the sum of the inverse of each of the components in series. Equation 28 is simplified to combine resistances into only three terms, those on the reaction side of the vessel wall ( $h_i$ ), the vessel wall ( $h_w$ ), and those on the jacket side of the vessel wall ( $h_o$ )

$$\frac{1}{U} = \frac{1}{h_o} + \frac{1}{h_w} + \frac{1}{h_i} \quad (28)$$

The sum of those resistances not relating to the reaction mixture (that is the terms for the wall and jacket side) is equal to a vessel constant (eq 29). This is called the Wilson intercept and is a valid assumption over a limited temperature range.

$$\frac{1}{h_w} + \frac{1}{h_o} = W_v \quad (29)$$

This constant can be easily measured for a given vessel using a method called a Wilson plot.

The method plots  $U^{-1}$  on the  $Y$  axis and  $(N/N_0)^{-2/3}$  on the  $X$  axis, where  $N$  is the agitation rate and  $N_0$  is a small reference

agitation rate where the internal heat transfer becomes zero. This is in practice just a small number. The heat transfer of the vessel is measured at four or five different agitation rates, and resulting values are plotted on a graph of  $U^{-1}$  vs  $(N/N_0)^{-2/3}$ . The data should lay on a line, the  $y$  intercept of which is the Wilson constant (eq 29). The next assumption we must make is that agitation in the large vessel can be accurately scaled down to the lab vessel. This assumption is based on the practical work of Machado in characterizing the Mettler AP01-0.5.<sup>10</sup> For the purposes of this method, constant power per unit volume is utilized to predict agitation rates in the lab vessel, based on the scale factor and large scale agitation rate.<sup>11,12</sup> Maintaining  $Tr_{\text{lab}} = Tr_{\text{scale}}$ , using equivalent agitation and identical reaction composition, ensures proportionality of  $h_{i \text{ scale}}$  and  $h_{i \text{ lab}}$ , as would be expected from a Dittus-Boelter-like correlation. This proportionality constant can be measured with a solvent test near the reaction volume and temperature of interest in both the lab reactor and the large scale reactor.

$$P * h_{i \text{ lab}} = h_{i \text{ scale}} \quad (30)$$

From eqs 28 and 29 we can solve for the heat transfer coefficient of the large scale reactor

$$U_{\text{scale}} = \frac{1}{\left( \frac{1}{h_{i \text{ scale}}} + W_{\text{scale}} \right)} \quad (31)$$

Substituting the proportionality of eq 30  $h_{i \text{ scale}}$  into eq 32:

$$U_{\text{scale}} = \frac{1}{\left( \frac{1}{P * h_{i \text{ lab}}} + W_{\text{scale}} \right)} \quad (32)$$

From eqs 28 and 29 we can solve for  $h_{i \text{ lab}}$  in the case of the lab reactor, as we did for the scale reactor in eq 33.

$$h_{i \text{ lab}} = \frac{1}{\left( \frac{1}{U_{\text{lab}}} - W_{\text{lab}} \right)} \quad (33)$$

Substituting the equality of  $h_{i \text{ lab}}$  in eq 33 into eq 32,  $U_{\text{scale}}$  can be expressed in terms of scale vessel constants and laboratory measurements.

$$U_{\text{scale}} = \left[ \left( P \left( \frac{1}{U_{\text{lab}}} - W_{\text{lab}} \right) \right)^{-1} + W_{\text{scale}} \right]^{-1} \quad (34)$$

Equation 34 is substituted into eq 27 wherever  $U_{\text{scale}}$  is used, resulting in eq 35. In eq 35,  $T_{j_{\text{lab}}}$  is now expressed as a function of easily measurable vessel constants and measurable real time lab variables, with the exception of  $T_j$  scale.

**Simulation of the Large Scale Reactor Jacket ( $T_j$  Scale).** Precise modeling of the large scale jacket would be an extremely complex operation involving numerous variables and equations. To precisely model jacket temperature, one would first model the controlling PID loop. Realizing that this loop just controls the flow of hot and cold media into a large mixing volume (the jacket recirculation loop), one must also account for valve operation delays, the temperature and flow rates of the hot, cold, and recirculation loop media, mixing dynamics within the jacket and recirculation loop, as well as any thermal transfers to the environment and the reaction mixture.

To simplify the task of simulating the large scale reactor

$$T_{j_{lab}} = \left[ 1 - \frac{\left[ \left( P \left( \frac{1}{U_{lab}} - W_{lab} \right)^{-1} \right)^{-1} + W_{scale} \right]^{-1} (A_{scale\ start} + \Delta m_{lab} Z)}{Sf * UA_{lab}} \right] Tr + \frac{\left[ \left( P \left( \frac{1}{U_{lab}} - W_{lab} \right)^{-1} \right)^{-1} + W_{scale} \right]^{-1} (A_{scale\ start} + \Delta m_{lab} Z)}{Sf * UA_{lab}} T_{j_{scale}} - C \quad (35)$$

jacket, we chose the following approximation method. Starting with the basic PID equation

$$T_{j_{scale\_unbounded}} = K_p(Tr - Tr_{set}) + K_i \int_{t_0}^{t_{reset}} (Tr - Tr_{set}) dt + \left( K_d \frac{d(Tr - Tr_{set})}{dt} \right) + Tr_{set} \quad (36)$$

where  $T_{j_{scale\_unbounded}}$  is a theoretical jacket response temperature,  $K_p$  is the proportional constant,  $K_i$  is the integral constant, and  $K_d$  is the derivative constant. The constants must be fitted to approximate a known jacket response. This was accomplished in a working commercial facility by fitting to past  $Tr$  and  $T_j$  trends produced during cleanings and solvent runs.

Equation 36 calculates a theoretical large vessel jacket temperature that is unconstrained by the realities of the actual vessel. Thus, the PID calculated  $T_j$  must be bounded by a minimum and a maximum possible jacket temperature, which is done in Excel utilizing limits entered by the user. A simple if/then statement is set up where the calculated temperature is reported if it falls between the upper or lower limit. If the calculated jacket temperature is less than or equal to the lower limit, the lower limit is reported; and if it is greater than or equal to the upper limit, the upper limit is reported.

One must also keep in mind that the PID loop of the large scale reactor is not directly controlling the jacket temperature but rather it is controlling the flow rates of hot and cold heat transfer media using proportional control valves. To approximate this reality,  $T_{j_{scale}}$  is further constrained by a maximum rate of temperature change. The large volume of jacket fluid in the recirculation loop will take time to change temperature given a limited in-flow and out-flow. Practically, this rate can be experimentally measured on the large vessel near the anticipated jacket temperature range of the reaction to be scaled down. The use of two rates of change, one for cooling and one for heating, more closely matched the real life jacket performance observed in all of the large scale vessels we modeled. An Excel macro was used to calculate the final simulated full scale jacket temperature incorporating all of the above calculations and constraints. Table 2 gives typical values that can be used as a starting point for the  $T_j$  scale simulation.

**Dynamic  $U_{scale}$  Correction Based on a Real Time  $U_{lab}$  Measurement.** A correction for changing heat transfer coefficient “ $U$ ” can be a valuable addition to this method when the reaction under study undergoes large physical property changes. Dynamic heat transfer requires the lab vessel to be a calorimeter capable of constantly measuring the laboratory heat transfer coefficient. Our method is readily

adaptable to real-time updating of the  $U_{lab}$  value with subsequent recalculation of  $U_{scale}$ , as previously described for the static case in eq 32.

**Table 2. Typical Starting PID Values**

max jacket heat rate	6–10 °C/min
max jacket cool rate	3–6 °C/min
integral reset	1–2 min
integral reset multiplier	0–0.4
$K_p$	2.5–10
$K_i$	2
$K_d$	2

**Implementation and Programming within Mettler iControl RC1e Software and Microsoft Excel.** Control of the reactor jacket temperature was accomplished using Mettler iC Data Share. This Excel add-in was in noncommercial beta release form at the time of this work. It has since been released as a commercial product. It functions by polling the iControl software for experimental variables such as mass, batch temperature, and heat transfer area and then communicating back calculated values such as  $T_j$  set point. A macro was set up on the I/O Excel sheet that polled the time value coming from iControl and recalculated the sheet to obtain a new  $T_j$  set point only when that cell had changed. This was necessary in setting up a PID loop to simulate the large scale jacket temperature.

## ■ EXPERIMENTAL SECTION

A number of preliminary measurements must necessarily be made to fully characterize the laboratory Mettler RC1 RTCal (AP01-0.5-3W) reactor and scale-up reactors.

**Characterization of a Prep-Scale Two Gallon Scale-up Vessel.** Wilson plots were utilized to characterize the shell side and wall resistance to heat transfer for a heat exchanger of the prep-scale vessel (Figure 1).

The vessel inside diameter and dish area and volume were ascertained from the vessel drawings. These were utilized to calculate the wetted surface area of a 4 L charge of toluene. A reference point was marked on the reactor at the unstirred liquid level. The liquid was cooled to 0 °C, and liquid level measurements from the reference level were taken at each of the intended agitation rates. The reactor was heated to 80 °C and the measurements repeated. This gave a virtual volume vs temperature correlation at each agitation rate. From this relationship, the wetted surface area can be determined for any temperature and agitation rate using surface area equations that describe the geometry of the vessel. (The dish of this reactor is jacketed. In most cases, “A” should only include the jacketed

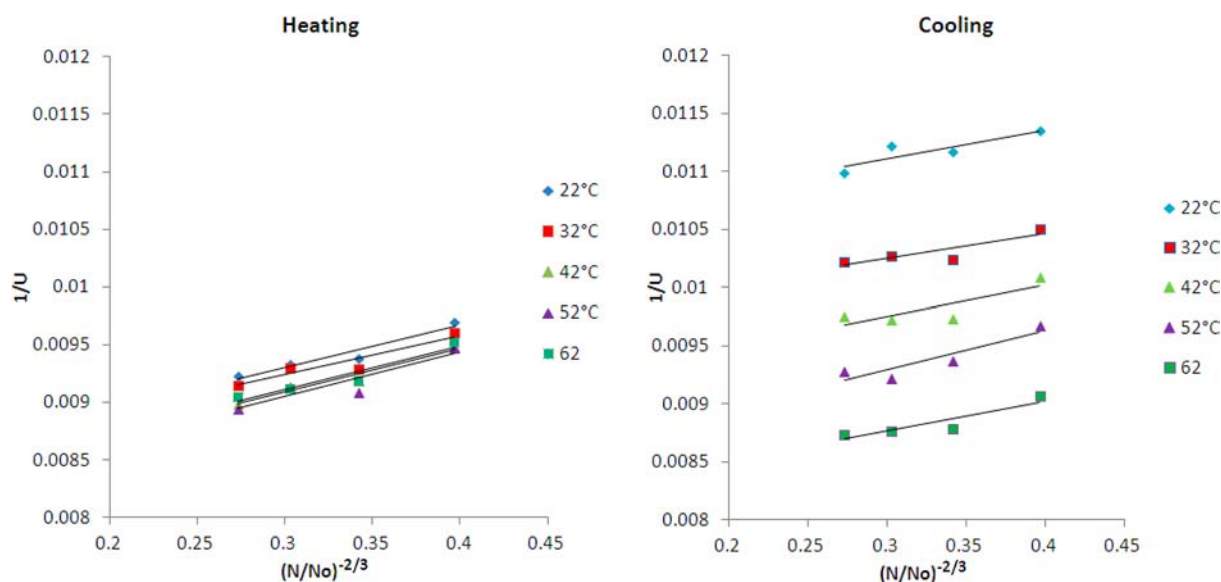


Figure 1. Wilson plots for proprietary 2-gallon vessel: Heating and cooling plots.

surface area beneath the liquid level.) The agitator was set to 100 rpm with the solvent temperature at 0 °C.  $T_r$  control was then set to 80 °C while  $T_r$  and  $T_j$  were recorded. Once the contents reached 80 °C,  $T_r$  control was set to 0 °C, recording  $T_r$  and  $T_j$  data until the contents reached 0 °C. This process was repeated for agitator speeds of 200, 250, 300, and 350 rpm. Data smoothing was employed, and only areas of the cycle where  $T_r - T_j$  was relatively stable and large were used in the calculations.

The heating data was much more tightly grouped than the cooling data. Note however from Table 3 that this made little difference in the external heat transfer coefficient values.

Table 3. Comparison of Heating and Cooling Heat Transfer Coefficients Measured at Various Temperatures in a Proprietary Design 2 Gallon Vessel

temp (°C)	cooling $U$ (W/(m <sup>2</sup> K))	heating $U$ (W/(m <sup>2</sup> K))	avg $U$ (W/(m <sup>2</sup> K))
22	96	122	108
32	104	122	112
42	112	126	118
52	121	127	124
62	125	125	125
avg 22–62	112	124	117

The external heat transfer coefficient for the 2 gallon = 117 W/(m<sup>2</sup> K), which is the average intercept of heating and cooling cycles at all measured agitation rates >100 rpm and all temperatures.

**Characterization of a Mettler AP01-0.5-3W Glass RTCal Reactor.** A Mettler RC1e MidTemp utilizing iControl 5.0 beta and equipped with an AP01-0.5-3W RTCal reactor, an agitator with two tiers of three pitched blades each, a calibration heater, and a Hastelloy-C baffle was charged with 250 mL of a suitable solvent. Heat transfer coefficients ( $U$ ) were determined using the calibration heater for 300, 500, 700, and 800 rpm of agitation at each temperature. 250 mL is our typical fill level and thus was chosen to represent the majority of our reaction conditions. The change in Wilson intercept as a function of temperature is a result of the temperature dependent viscosity

change of the Mettler MidTemp oil used in the jacket (Figure 2).

Reactor fill level was also explored as a variable and found to hold to the same Wilson intercept values as long as the fill remained above 250 mL. There was a significant decrease in the Wilson intercept below the 250 mL fill level. This result is not unexpected, as the sensor probes begin to lose sufficient liquid coverage at approximately 200 mL fills.

**Case Study 1: Scale-Down of a Rapid Addition Dose-Controlled Reaction.** The process to produce kilo quantities of a pharmaceutical intermediate called for the rapid addition of a reagent to a stirring mixture, resulting in a modest amount of precipitate formation. This acid–base reaction is dose-controlled even at very rapid addition rates.

Could this process be scaled up 13-fold into a 2 gallon reactor? It is possible to accurately predict the maximum batch temperature utilizing a dose-controlled heat transfer scale-up model. However, because of the large temperature increase, such a model may not adequately predict the actual scale-up effects on variables such as product quality and byproduct formation. Figure 3 depicts the actual 2 gallon reaction (in gold and purple) with the first attempt at scale-down simulation overlaid (in red and black). The  $T_{j, \text{scale}}$  algorithm used in this simulation was proportional control only.

The scale-down reaction temperature prediction curve (in red) and the actual scale-up reaction temperature (in gold) are in very good agreement. The maximum predicted internal temperature is within a few tenths of a degree of the actual scale-up batch temperature, i.e. a prediction error on the heat rise of less than one percent. However, early in the run, there is a rapid decline in the lab reaction temperature relative to the scale-up run reaction temperature. The scale-down internal temperature curve deviates by as much as 10 °C from the 2 gal internal temperature curve due to the scale-down reactor's jacket response time to set point changes. This is visualized in Figure 4 by the difference between the lab reactor jacket temperature (in green) and the lab reactor set point (in blue). This difference caused an increase in lab scale heat transfer that resulted in  $T_r$  lab deviating from  $T_r$  scale. The lab scale jacket response time is a limitation of the method and must be considered when simulating large rapid reaction temperature

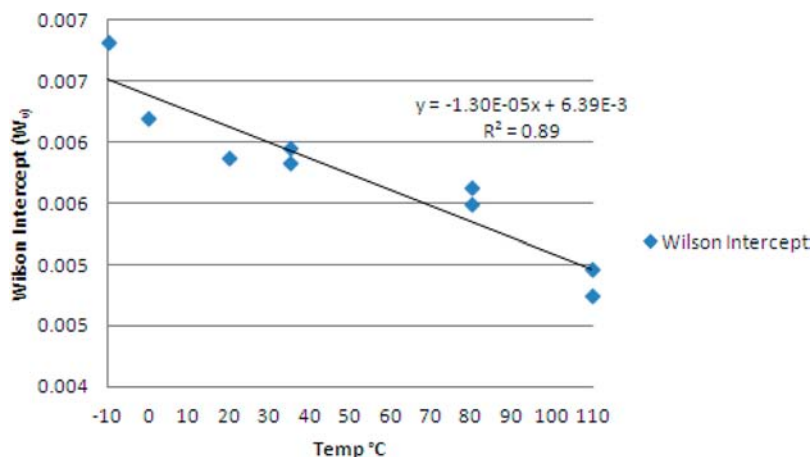


Figure 2. AP01-0.5-3W Wilson intercept vs temperature.

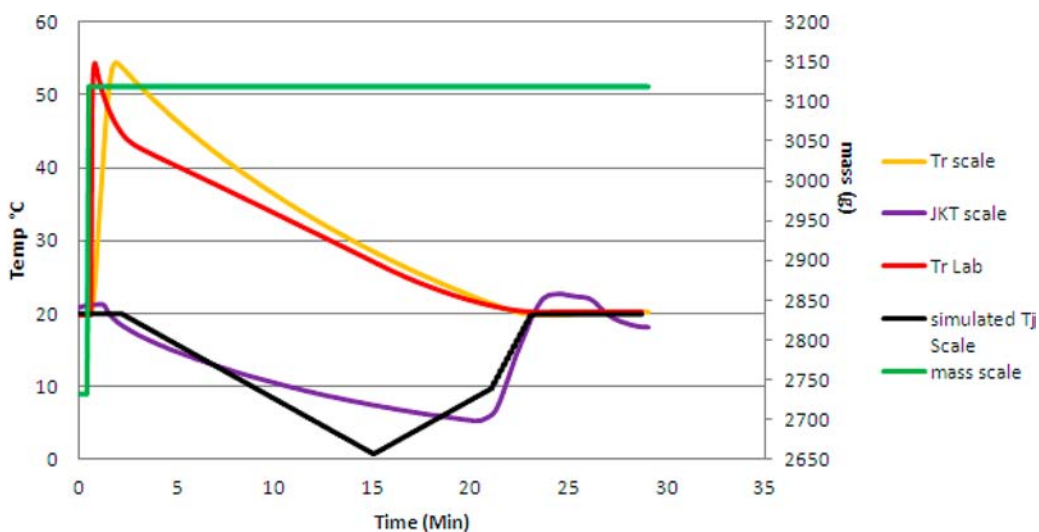


Figure 3. Case 1: Overlay of actual scale-up run and lab scale-down first attempt simulation.

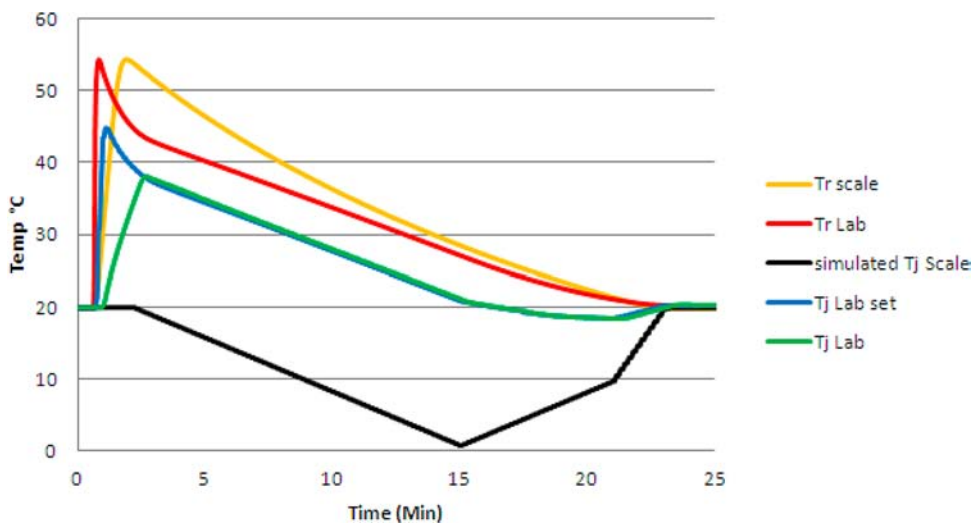


Figure 4. Case 1: Overlay of lab  $T_j$ ,  $T_j$  set point with  $Tr$  lab,  $Tr$  scale, and simulated  $T_j$  scale

changes. Because the scale jacket response and the simulated scale jacket response differed significantly in the above trial, the scale vessel jacket simulation algorithm was changed to the current full PID control and a smaller maximum cooling rate

was used. Figure 5 depicts the same large scale run overlaid with a new lab run using a full PID loop large scale jacket temperature simulation.



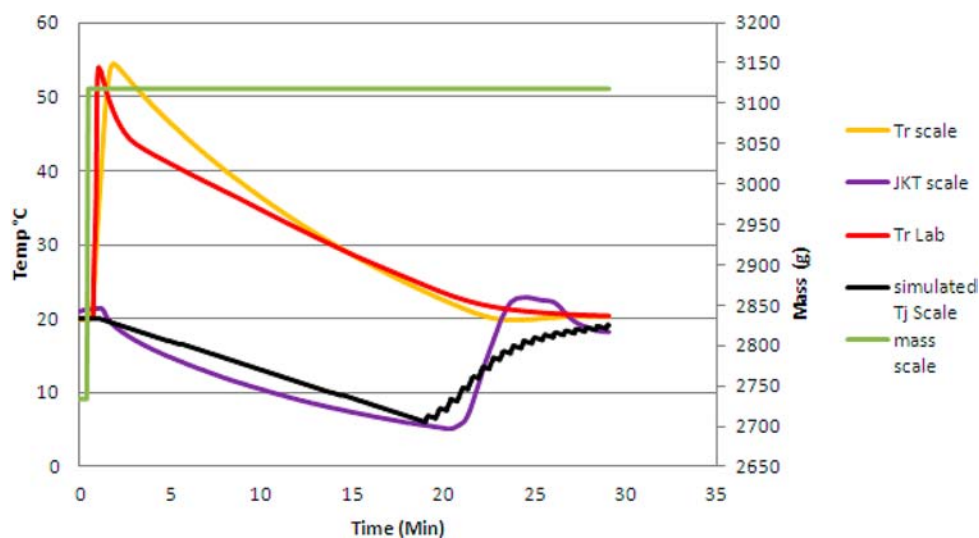


Figure 5. Case 1: Overlay of actual scale-up run and lab scale-down simulation second run.

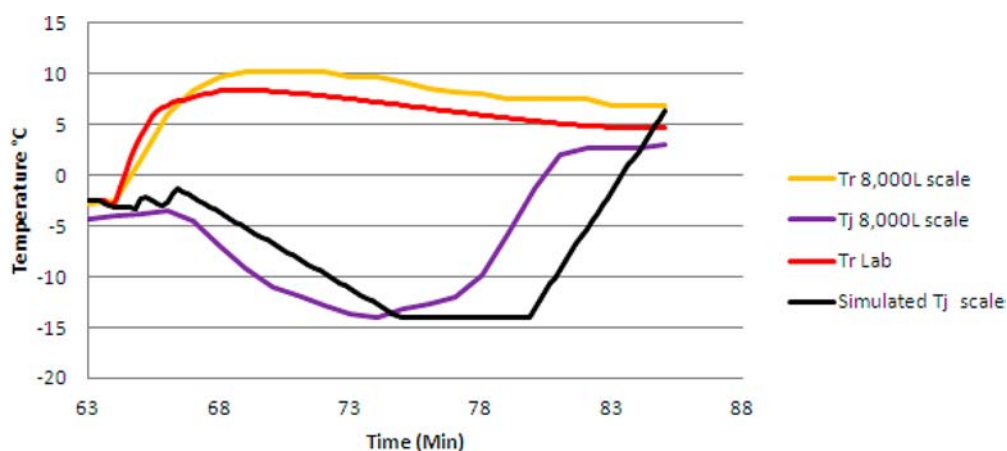


Figure 6. Case 2: Overlay of actual scale-up run and lab scale-down simulation.

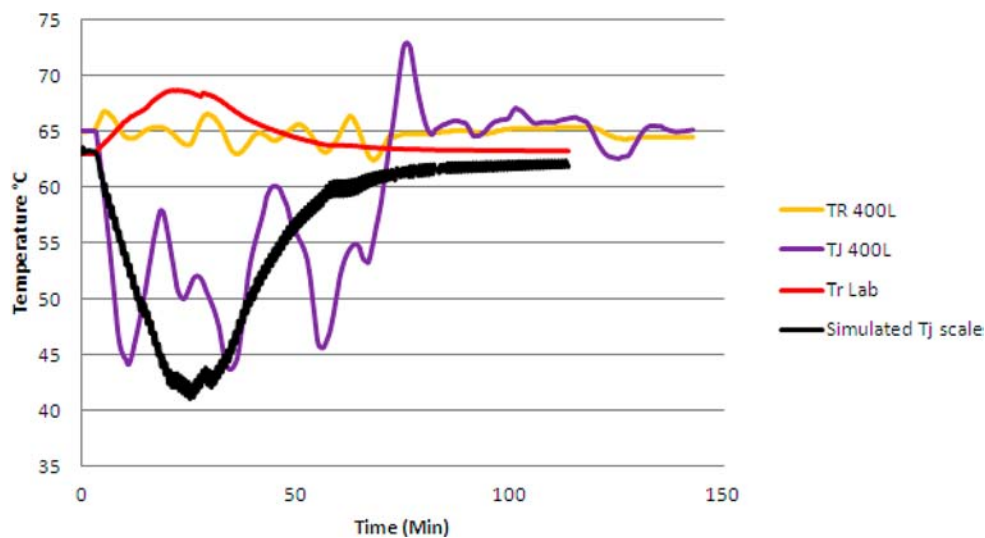


Figure 7. Case 3: Overlay of actual scale-up run and lab scale-down simulation.

The robustness of the predictions made by this method is demonstrated in this case study. The simulated scale jacket response does not have to fit perfectly to get a good prediction of the on-scale reaction temperature. The large scale maximum

reaction temperature was predicted to within a few tenths of a degree, utilizing either jacket simulation method. The reaction temperature maxima occur at slightly different times. This is explained by dosing rate differences and thermocouple

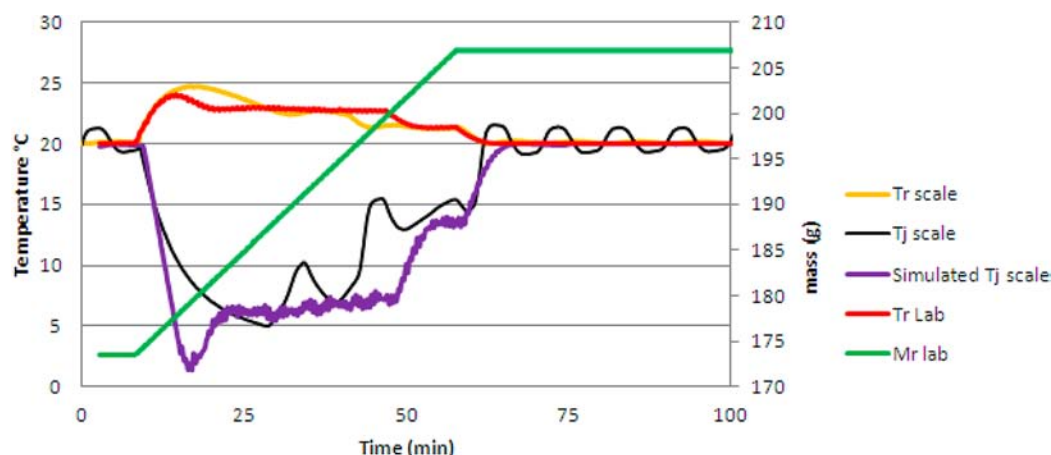


Figure 8. Case 4: Overlay of actual scale-up run and lab scale-down simulation.

response times. The thermocouple on the large vessel has a longer response time, and thus the curve maximum on the  $Tr_{scale}$  trend falls about 90 s after the  $Tr_{lab}$  trend maximum.

**Case Study 2: Nondose Controlled Pharmaceutical Intermediate Formation.** The following example is a simulation of a 200 kg batch ( $Sf = 4300$ ) of pharmaceutical intermediate that exhibits a nondose controlled exotherm. This process has a proposed mechanism that involves four separate reactions and several radical changes in reaction viscosity resulting from heavy precipitations followed by partial dissolution of the solids. The resulting radical heat transfer coefficient changes, reaction temperature changes, and nondose controlled nature of this process excluded the use of traditional dose control  $Qr$  based computer models. On smaller pilot plant scale, this batch nearly exceeded temperature limits. Earlier iterations of the scale-down simulation predicted that the 200 kg batch would indeed exceed the upper temperature specification as the process was currently run. Adjustments were made to the process, and the scale-down model was rerun to give the prediction shown in Figure 6. On scale-up the actual 200 kg reaction temperature and jacket temperatures are denoted by the gold and purple trends. The scale-down model predicted the maximum reaction temperature to be 8.4 °C. The scale-up batch barely maintained the temperature range  $-5$  to 10 °C, with a maximum reaction temperature of 10.4 °C. Future scale batches were started at a slightly lower temperature to allow for a wider margin of error. It is important to note that this scale-down method predicts the internal temperature–time profile that would be observed at scale. The predictive ability of this method allows for realistic impurity generation stress studies, which can be extremely helpful in both parameter criticality assessment and technology transfer. Thus, process parameters, such as reaction temperature, dose rate, etc., can be varied in lab stress studies taking both equipment capability and process capability into account.

**Case Study 3: Scale-Down of a Complex Multiphase, Nondose Controlled Reaction.** Figure 7 shows the complex nondose controlled reaction used to produce a pharmaceutical intermediate in 250 gal scale compared with the scale-down prediction in red. The predicted maximum temperature of 68 °C is 2 °C or only 3% higher than the maximum temperature observed at scale (in gold). It should be noted that limited data on the toll manufacturer's vessel was available prior to the production run. The vessel heat transfer coefficient was estimated using a commercially available computer model,

and the vessel jacket response was fitted to data from a similar size vessel in one of our plants. The variations in the scale-up vessel's jacket temperature in Figure 7 are due to operator-controlled manual valves making computer simulation of the jacket temperature profile challenging. Despite these issues, it is noteworthy that the scale-down method proved quite predictive of the  $Tr_{scale}$  trend observed upon scale-up.

The deviation of the final temperatures is explained by the lab vessel set point being placed at the midpoint of the acceptable range while the plant operator maintained a batch temperature near the upper limit of the specified temperature range.

**Case Study 4: Scale-Down of a Slow Addition Dose-Controlled Reaction.** The maximum reaction temperature for a 13-fold scale-up was required for the production of a starting material. The RC1 dosing loop was set for 50 min, as this was the desired addition time on scale. The scale-down model predicted a maximum reaction temperature of 24 °C. This dosing time was then utilized in a proprietary design 2 gallon reactor during the performance of the actual run. The large scale vessel reached a maximum reaction temperature of 24.9 °C. The scale-down run predicted a maximum temperature 0.9 °C below the actual scale run within  $\pm 5\%$  of the actual value. This can easily be explained by the difference in behavior between the simulated and actual scale jackets. Note that the simulated jacket (Figure 8: black trend) reacted faster and went to a significantly lower temperature during the initial exotherm where  $Tr_{max}$  occurs.

## CONCLUSIONS

We have demonstrated both the first principles derivation and practical application of a computer-controlled experimental scale-down procedure based on controlling heat transfer utilizing a lab vessel's jacket set point. This method has distinct advantages in computational simplicity over previously reported methods that calculate and control the lab reactor reaction temperature set point utilizing real-time heat flow calculations. Unlike scale-up models commonly used, this method is capable of predicting reaction temperature profiles for both dose-controlled and nondose controlled reactions over a wide range of changing reaction conditions. For nondose-controlled reactions, this method provides a direct prediction of internal temperature at scale without estimating reaction kinetics. The most exciting utility of this method is that it can be used to assess manufacturability of reactions or reaction schemes early

in the route selection process, long before a detailed kinetic or mechanistic understanding of the process is available. Reactions identified as hard to control on scale can either be discarded early or receive early reaction engineering support, contributing to the inherent safety of the developed processes. Because the reaction temperature profile mimics the scale-up temperature profile, the result of manufacturing process changes on reaction temperature and impurity profile can be studied much more realistically on laboratory scale than has been previously possible with computer simulations or previous scale-down methods. This allows for more aggressive scale-up of processes into production facilities and greater understanding of the scale dependent effects of process changes. A potential extension of this scale-down method would utilize a library of scale-up vessel-specific control parameters, thereby introducing a much needed connectivity between process control employed in the lab and manufacturing. Utilizing this method, what-if scenarios can be easily studied and consequences as to safety, reaction temperature, quality, reaction time, dosing times, gas evolution, and much more can be quantified on small scale long before a process reaches production or even pilot scale. In the future, we plan to extend this approach to predict temperature–time profiles for jacketed separation process equipment, such as jacketed filters and dryers.

Although this method was demonstrated in a reaction calorimeter, the method mathematically does not require the measurement of heat flow data to function and thus can be run in any computer-controlled jacketed reactor for which the appropriate vessel constants are known.

## ■ ASSOCIATED CONTENT

### 📄 Supporting Information

Excel macro to calculate a simulated  $T_j$  scale and scale-down set-points; summary of equations and terms; data tables for Wilson plots in the experimental section; and a line by line derivation of  $Tr_{lab} = Tr_{scale}$ . This material is available free of charge via the Internet at <http://pubs.acs.org>.

## ■ AUTHOR INFORMATION

### Corresponding Author

\*E-mail: [dryf1@sbcglobal.net](mailto:dryf1@sbcglobal.net)

### Notes

The authors declare no competing financial interest.

## ■ ACKNOWLEDGMENTS

The authors acknowledge the contributions of Vaidyaraman Shankarraman in coding the Excel  $T_j$  scale macro. We thank Leen Schellekens and the technical support staff at Mettler Toledo Autochem for the many hours of consultation on the functional details of the iControl software as well as Nilesh Shah of Mettler Toledo Autochem for making available the custom interface connection between Excel and iControl (later to become iC Data Share) that enabled this project to move from an idea to reality. We also acknowledge the efforts of Jeff Niemeier and Sean Lapekas for hours spent editing, proof-reading, and equation checking.

## ■ REFERENCES

(1) Sharkey, J. J.; Cutro, R. S.; Fraser, W. J.; Wildman, G. T. Process Safety Testing Program for Reducing Risks Associated With Large Scale Chemical Manufacturing Operations. *Plant/Oper. Prog.* **1992**, *11*, 238–246.

(2) Landau, R. N.; Williams, L. R. Reaction Calorimetry: A Powerful Tool. *Chem. Eng. Prog.* **1991** December.

(3) Mettler Toledo Autochem. *iControl RC1e Help Guide*, Version 5.0; Mettler-Toledo AG, AutoChem: Schwerzenbach, Switzerland, 2011.

(4) Regenass, W. Thermal and Kinetic Design Data from Bench-Scale Heat Flow Calorimeter. *ACS Symp. Ser.* **1978**, *65*, 37.

(5) Niemeier, Jeffrey Using Dynochem to Scale Up Data from Various Calorimeters. Presented at DynoChem 2009 User's Meeting Philadelphia, May 13–14, 2009.

(6) Leen Schellekens. Mettler-Toledo Autochem, Millersville, MD. Personal communication, 2010 of Mettler-Toledo Application Feasibility Scaledown work in RC1e at Wyeth Montreal, Canada. Performed by C. Benhaim, Senior Research Scientist Wyeth, Montreal, Canada, and S. Rea Senior Technology & Application Consultant Mettler-Toledo AutoChem Inc.

(7) Zufferey, B. Scale-down Approach: Chemical Process Optimization Using Reaction Calorimetry for the Experimental Simulation of Industrial Reactors Dynamics. Ph.D. Thesis, Ecole Polytechnique Federale De Lausanne, 2006.

(8) Zufferey, B.; Stoessel F.; Groth U. Method for simulating a process plant at laboratory scale. U.S. Pat. Appl. 11/530,928, 2007.

(9) Rose, J. W. Heat-Transfer Coefficients, Wilson Plots and Accuracy of Thermal Measurements. *Exp. Therm. Fluid Sci.* **2004**, *28*, 77–86.

(10) Machado, R. R. *Mettler Toledo iControl Mixing Guide 5.0*; Mettler-Toledo AG, AutoChem: Schwerzenbach, Switzerland, 2010.

(11) Paul, E. L.; Atiemo-Obeng, V. A.; Kresta, S. M. Mechanically Stirred Vessels. *Handbook of Industrial Mixing Science and Practice*; John Wiley & Sons: Hoboken, NJ, 2004; pp 376–378.

(12) Oldshue, J. Y. *Fluid Mixing Technology*; McGraw-Hill Publications: New York, NY, 1983; pp 1–71.